LBL-32164
UC-404

Lawrence Berkeley Laboratory
UNIVERSITY OF CALIFORNIA

Materials Sciences Division

Presented at the TMS Annual Meeting, San Diego, CA, March 2-5, 1992,
and to be published in the Proceedings

Statics and Kinetics of Oxygen Ordering in the Oxide Superconductor $YBa_2Cu_3O_z$

D. de Fontaine, R. McCormack, G. Ceder, and E. Salomons

March 1992

LOAN COPY
Circulates
for 4 weeks
Bldg. 50 Library.
Copy 2
LBL-32164

Prepared for the U.S. Department of Energy under Contract Number DE-AC03-76SF00098

DISCLAIMER

This document was prepared as an account of work sponsored by the United States Government. While this document is believed to contain correct information, neither the United States Government nor any agency thereof, nor the Regents of the University of California, nor any of their employees, makes any warranty, express or implied, or assumes any legal responsibility for the accuracy, completeness, or usefulness of any information, apparatus, product, or process disclosed, or represents that its use would not infringe privately owned rights. Reference herein to any specific commercial product, process, or service by its trade name, trademark, manufacturer, or otherwise, does not necessarily constitute or imply its endorsement, recommendation, or favoring by the United States Government or any agency thereof, or the Regents of the University of California. The views and opinions of authors expressed herein do not necessarily state or reflect those of the United States Government or any agency thereof or the Regents of the University of California.

STATICS AND KINETICS OF OXYGEN ORDERING

IN THE OXIDE SUPERCONDUCTOR $YBa_2Cu_3O_z$

D. de Fontaine[1,2], R. McCormack[1], G. Ceder[3] and E. Salomons[4]

[1]Department of Materials Science and Mineral Engineering, University of California, Berkeley, CA 94720, USA
[2]Materials Sciences Division, Lawrence Berkeley Laboratory, Berkeley, CA 94720, USA
[3]Department of Materials Science and Engineering, Massachusetts Institute of Technology, Cambridge, MA 01239, USA
[4]CEN Saclay, 91191 Gif-sur-Yvette, France

Abstract

Oxygen ordering in the high-temperature superconductor $YBa_2Cu_3O_z$ is well described by a two-dimensional Ising model with anisotropic next-nearest neighbor effective pair interactions, repulsive along the *a* direction, attractive along *b*. Monte Carlo simulation shows that this marked anisotropy gives rise, particularly at stoichiometric index z close to 7, to large deviations from unity of the ratio D^*_{11}/D^*_{22} of tracer diffusion tensor components in the *a* and *b* directions. Oxygen ordering kinetics are shown to evolve in a manner which parallels those of the experimentally observed increase with aging time of the superconducting transition temperature for $z<7$.

This work was supported by the Director, Office of Energy Research, Office of Basic Energy Sciences, Materials Sciences Division of the U.S. Department of Energy under Contract No. DE-AC03-76SF00098.

Introduction

The problem of oxygen ordering in the superconducting compound $YBa_2Cu_3O_z$ (YBCO) has attracted considerable attention not only because of its intrinsic scientific interest, but also because oxygen ordering has been shown to be intimately related to the phenomenon of high-temperature superconductivity. In this mini-review, we shall summarize the original model proposed for oxygen ordering in YBCO, the so-called Asymmetric Next Nearest Neighbor Ising (ASYNNNI) model. The choice of *asymmetric effective pair interactions* is by no means arbitrary but can be rationalized on theoretical grounds and confirmed by first-principles electronic structure calculations. In what follows, we shall describe the model, then work out its consequences for both the statics and kinetics of oxygen ordering. The calculated phase diagram agrees remarkably well with experimental data, and Monte Carlo simulation provides information not only about oxygen tracer diffusion in this system, but also about the relationship between oxygen ordering and the phenomenon of superconductivity itself. We shall also take this opportunity to dispel some erroneous notions which have unfortunately worked their way into recent literature on the subject.

1. The Model

The model proposed [1] for describing the thermodynamics of oxygen ordering in YBCO regards the "chain" plane as a two-dimensional Ising model with a repulsive first-neighbor effective pair interaction (EPI), denoted V_1, and second neighbor effective interactions which take on different values depending upon whether the interaction is mediated by an intervening Cu ion or not. These interactions, denoted by V_2 and V_3, respectively, are depicted in Fig. 1. The ground states of order were determined rigorously [2] for all possible ratios V_2/V_1, V_3/V_1 ($V_1>0$), and were later rederived analytically [3]. In YBCO, it was soon ascertained that the V_n effective interactions had to obey the following inequalities:

$$V_2 < 0 < V_3 < V_1 \tag{1}$$

in order to represent the YBCO system accurately. Inequalities (1) can be rationalized easily on physical and chemical grounds, as will be shown presently. First-principles calculations [4] also gave values of V_1, V_2 and V_3 which satisfied (1).

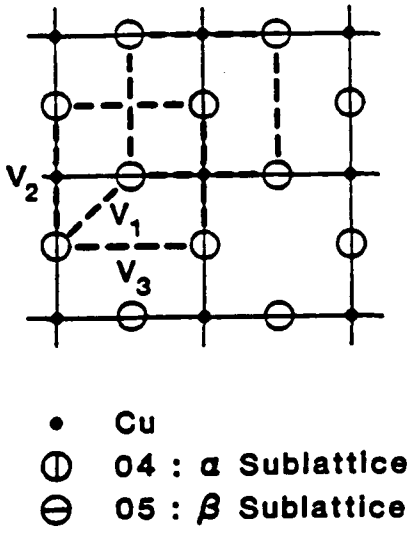

Figure 1 - Model for the $YBa_2Cu_3O_z$ basal plane.

The first acceptable oxygen-ordering phase diagrams for YBCO were calculated independently by Zubkus et al. [5] and by Kikuchi and Choi [6], with, as input to the cluster variation method (CVM), phenomenological interactions obeying inequalities (1). A very similar CVM calculation [7] was then performed with the V_n parameters derived from LMTO (linear muffin-tin orbital) electronic structure computations [4] (see Fig. 2, to be described in more detail below). Despite the fact that no fitting parameters were used in the phase diagram calculations, agreement with available experimental data (filled circles on transition line, [8]) was remarkably good. Very recently, accurate transfer matrix techniques were used to retrofit the V_n effective pair interactions to a large set of tetragonal ↔ orthorhombic transition data [9]. As expected, the resulting V_1, V_2, V_3 satisfied inequalities (1). The case for the general correctness of the asymmetric next nearest neighbor Ising ASYNNNI model thus appears to be a very strong one indeed.

The case is even more compelling on theoretical grounds. To show this, it is necessary to recall how effective pair interactions, more generally *effective cluster interactions* (ECI), are to be calculated theoretically. A rigorous definition of ECI's was first presented by Sanchez, Ducastelle and Gratias [10]. Recently, various computational schemes for deriving the ECI's were examined in detail, and the convergence of the interactions was studied numerically on model systems [11,12]. These theoretical studies provide clear definitions of the ECI; in particular, effective pair interactions V_n are given by (for the present case of filled "O" sites and vacant "❑" sites in the chain plane of YBCO):

$$V_n = \frac{1}{4}\left(W_{OO}^{(n)} + W_{\square\square}^{(n)} - W_{O\square}^{(n)} - W_{\square O}^{(n)}\right) \tag{2}$$

where $W_{OO}^{(n)}$ denotes the energy of two filled (O) sites in nth-neighbor pair position surrounded by a random distribution of O and ❑ sites, with similar definitions for ❑ - ❑ and O - ❑ pairs. Note, from this definition, that the V_n are completely symmetric in the interchange of filled and vacant sites. The energies W can, in principle, be calculated rigorously by quantum mechanical methods, and are of the order of the cohesive energy of the material. By contrast, the effective interactions result from the delicate balance between the positive and negative contributions in Eq. (2). As a result, the EPI's are orders of magnitude smaller than the corresponding W energies, and can be positive (repulsive) or negative (attractive), depending on the sign of the algebraic sum in Eq. (1).

In the YBCO case, the *signs* of V_1, V_2, and V_3 can be determined without performing any calculations. Due to electrostatic repulsion, "like" nearest neighbor pair energies ($W_{OO}^{(n)}$, $W_{\square\square}^{(n)}$) are necessarily higher than the "unlike" pair energies ($W_{O\square}^{(n)} = W_{\square O}^{(n)}$). Hence, V_1 is certainly positive. For the same reason, the *direct* second-neighbor interaction, V_3, must be positive, although, because the pair spacing is greater, it is probably smaller than V_1. The *indirect* effective interaction V_2 is of quite a different nature: strong O-Cu attraction, brought about by Cu d-orbital and O p-orbital coupling, clearly favors O-Cu-O configurations. It follows, unambiguously, that the effective interaction V_2 must be negative. It is the attractive V_2 interaction which stabilizes the O-Cu-O chains, a prominent feature of the YBCO compounds.

In the actual structure, "apical" (O4) sites are situated just above and below the Cu ions of the chains. The O4 sites are generally occupied so that the most probable O-coordinations around Cu are those indicated in Fig. 3. From the signs of the V_1, V_2, V_3 interactions, it follows that 4-fold (filled chains) and 2-fold (empty chains) coordination will be energetically favored, and the 3-fold coordination (chain end) will be unfavorable. Extensive tight-binding calculations by Burdett and Kulkarni [13] have confirmed that the 3-fold configuration has higher energy than the other two. Inequalities (1) thus represent algebraically the geometrical principle that Cu prefers either square-planar coordination or 2-fold "apical" coordination. In a recent publication [14], the authors have shown that 3-fold coordination (chain ends) tends to reduce hole count in YBCO and thus tends to depress T_c (see Section 5).

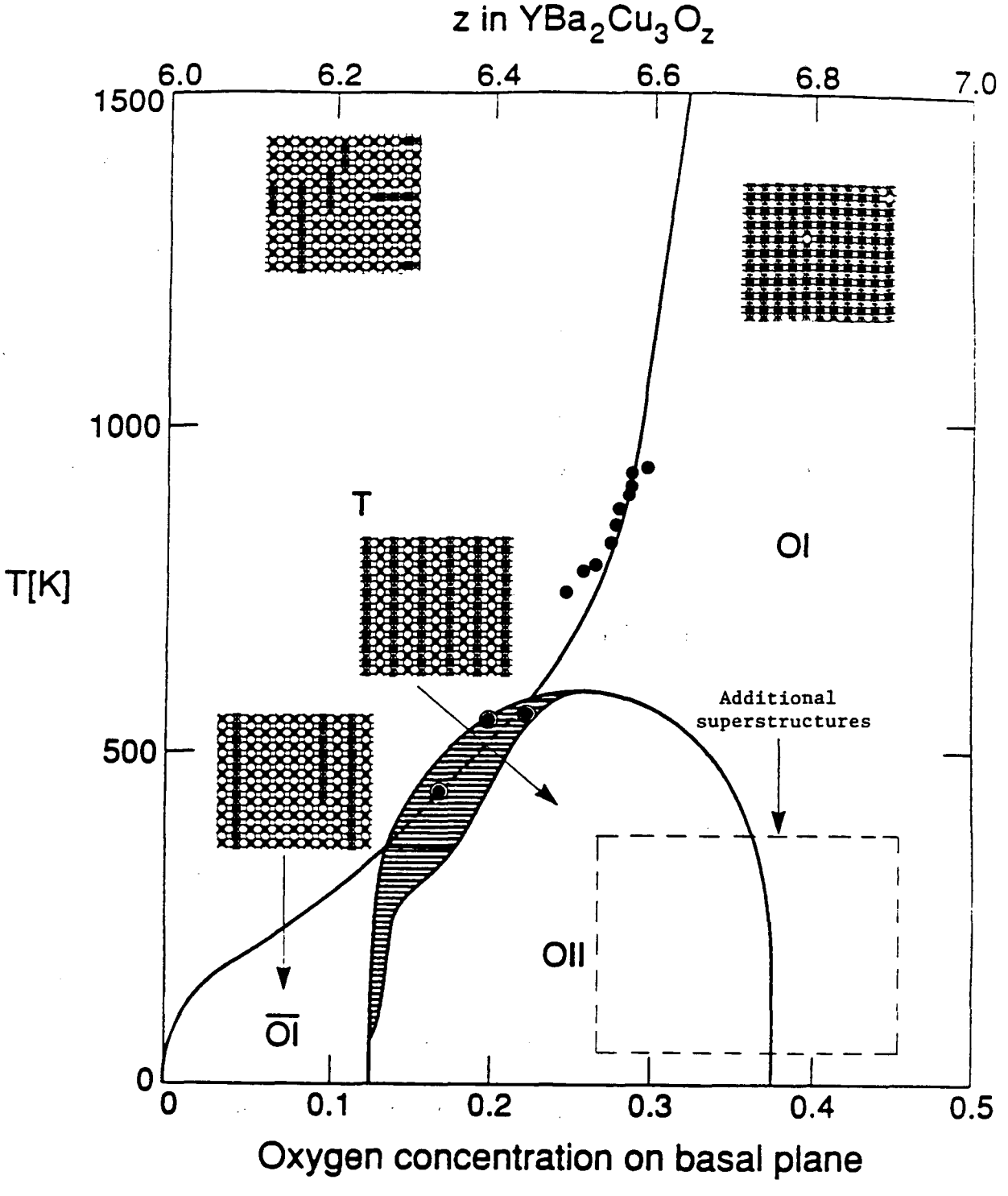

Figure 2 - Phase diagram using the CVM approximation for parameters calculated by Sterne and Wille (full lines). Experimental points (filled circles) from Andersen et al. Inserted structure diagrams were obtained from Monte Carlo simulations (small filled circles in inserts denote copper ions, large filled circles denote oxygen ions, and open circles denote vacant sites).

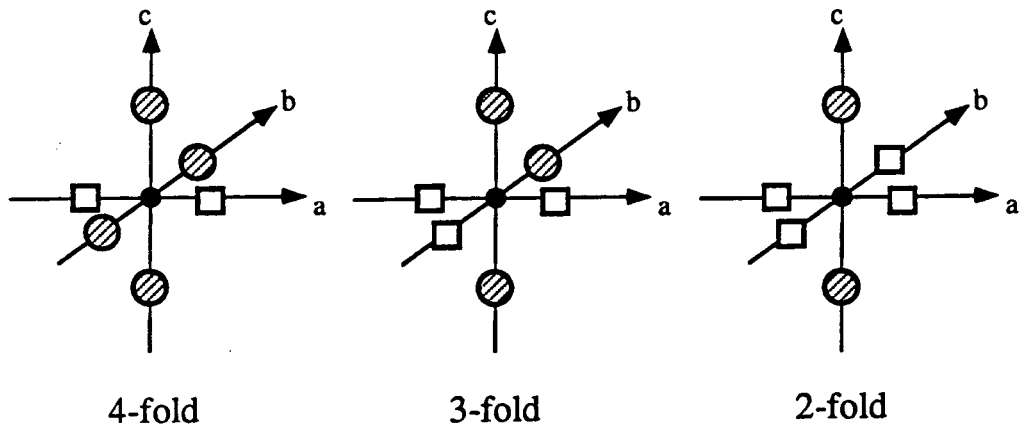

Figure 3 - The important configurations of oxygen around a Cu1 atom. It is assumed that the axial oxygens (along the c-axis) are always in place. Here, as elsewhere, small filled circles are Cu atoms, large shaded circles are O atoms.

These very simple considerations justify the ASYNNNI model in a most straightforward manner. It is therefore surprising that other models have been adopted which violate inequalities (1). For example, the equality $V_2 = V_3$ has been proposed, which necessarily robs this (symmetric) model of physical content and leads inevitably to the wrong structures and the wrong phase diagram [15,16]. In more recent work, however, Semenovskaya and Khachaturyan [17] appear to have adopted an asymmetric model [satisfying inequalities (1)], attributed incorrectly to Aligia and co-workers [18]. This model, which relies on (screened) Coulomb interactions, is based on the formula $V_n = V \exp(R_n/\lambda)/R_n$, where V is some unscreened potential, R_n is the nth neighbor pair spacing and λ is the screening length. Unfortunately, this formula gives (in our notation) $V_2 = V_3$ and hence is unacceptable. Aligia et al. are thus compelled to introduce an arbitrary factor f for the V_2 (Cu-mediated) interaction: $V_2 \rightarrow fV_2$ with $f<1$. For most thermodynamic work, Aligia et al. retain only three non-zero interactions, which means that three adjustable parameters, V, λ and f, are available for fitting purposes. The factor f is taken as positive or negative depending on the data to be fitted. Not surprisingly, any observed structure, stable or not, can be "explained" by this very tolerant model.

The real problem with the Aligia model lies deeper, however: it appears to confuse the terms "interatomic potential" (such as a Coulomb interaction) and "effective interaction" as defined by Eq. (2). As shown in detail elsewhere [10,11,12], it is the latter effective interaction V_n, obtained from Eq. (2), which must appear in structure determination and thermodynamic calculations. The Coulomb repulsion equation gives "potentials" which, if calculated properly, are orders of magnitude too large, are all positive, are "symmetric" ($V_2 = V_3$), and decay too slowly with pair spacing. The model is thus fundamentally incorrect and only appears to give the right answer because there are always enough adjustable parameters to fit any data that come along.

In the correct approach, that of Eq. (2), the small magnitude of the V_n is obtained as a difference of large numbers W, and negative values for the interactions appear naturally, in contrast to the "screened Coulomb potential" method just described. Moreover, a heuristic argument [12] shows clearly that for large pair spacings, the cancellation of W's in Eq. (2) will be almost perfect so that the V_n sequence will converge rapidly with increasing index n, much faster than "screened Coulomb interactions". Surely, Coulomb interactions (repulsive *and* attractive) play a role, but only as an ingredient in the computation of the individual W energies. In fact, these energy terms include a significant Madelung contribution; for the case of V_2, the dominant electrostatic contribution is a negative one from the nearest Cu-O pair, with a lesser (positive) contribution from the O-O second neighbor pair of ions. The resulting net effective interaction must necessarily be a negative (attractive) one for V_2. Interactions with other ions, Ba for example, also must be considered, of course, and are automatically included in the LMTO calculation mentioned above.

2. Equilibrium Phase Diagram

Let us now examine more closely the phase diagram of the ASYNNNI model predicted in the CVM approximation, with electronic structure-derived parameters [4] $V_1 = 6.9$ mRy, $V_2 = -2.4$ mRy, $V_3 = 1.1$ mRy. In Fig. 2, actual absolute temperature (in K) is plotted against oxygen concentration in the chain plane (lower scale, from 0 to 0.5). If no other oxygen sites in the three-dimensional YBCO are vacant, this scale is linearly related to the oxygen index z (upper scale, from 6 to 7). There is a line of continuous transitions which separates the tetragonal phase (T) from the orthorhombic phase (OI). In this particular calculation, the second-order transition line is interrupted by a narrow two-phase region, indicated in Fig. 2 by horizontal tie lines. This feature of the phase diagram does depend on the nature of the CVM entropy approximation and on the choice of interaction parameters. Inserted structure diagrams were obtained from Monte Carlo simulations with the parameters V_1, V_2, V_3 identical to those used for calculating the phase diagram. OI, at close to z = 7 stoichiometry, consists of predominantly filled O-Cu-O parallel chains (most of the sites on the α sublattice of Fig. 1 filled). OII has every other parallel chain empty (❑-Cu-❑) and $\overline{\text{OI}}$ consists of filled parallel chains in a predominantly "empty" background. The tetragonal phase consists of a random dispersion of fluctuating chain segments running statistically in two orthogonal directions. The $\overline{\text{OI}}$ phase, though not observed unambiguously, must exist for symmetry reasons at T=0 [7], although some investigators [19] have claimed that it is an artifact of the CVM approximation. In more recent and very detailed work by these investigators [9], $\overline{\text{OI}}$ appears clearly, however, although it is not labeled as such in their calculated phase diagram. For pair interactions limited to second neighbor pairs, the $\overline{\text{OI}}$ phase *must* be the stable one at low enough oxygen content and low (but non-zero) temperature: the internal energy can always be lowered by forming the longest possible parallel chains of O and Cu atoms.

The V_1, V_2, V_3 values used as input to the CVM phase diagram calculations leading to Fig. 2 were obtained by an inversion method [4] applied to superstructure energies obtained from LMTO computations. Despite the fact that not a single adjustable parameter was used, the agreement with experimental tetragonal $\leftrightarrow$ orthorhombic transition points [8] (full circles) is striking. It follows that one cannot arbitrarily tamper with V_n values and hope to retain this remarkable agreement; in particular, choosing a set of V_n which violates inequalities (1) will likely have disastrous effects on the phase diagram.

3. Additional Superstructures

Two major assumptions have been made in the calculations: (a) only three interactions have been used and (b) the V_n are assumed to be concentration-independent over the (0, 0.5) oxygen concentration interval. The concentration-independence of the interactions can be justified theoretically [11,12], but the neglect of higher neighbor pairs and "cluster" interactions is an approximation based on rapid convergence of the ECI, which is itself based on the cancellation of W terms in expression (2). However, longer-range interactions do exist, even if their relative magnitudes may be quite small. Additional ordered oxygen superstructures are thus

expected at low temperatures. The most significant of these interactions are expected to be repulsive ones normal to the chains. The search for corresponding ground states then practically reduces to determining one-dimensional ground states of mutually repelling objects, O-Cu-O chains in the present case. The exact solution to that problem (for "convex" interactions) is known [20], and the application to the YBCO case has been described elsewhere [21]. The hierarchy of resulting structures can be obtained by a simple algorithm, but the corresponding phase equilibria are very difficult to determine. Thus far, only the OIII phase boundaries have been calculated [22]. The region of the phase diagram where these long-period superstructures are expected in indicated by a dashed box in Fig. 2. The important point to note is that these structures *must be ground states*; it was shown [23] that they could not result, as was initially conjectured [16], as transients following spinodal decomposition.

A similar "box" of one-dimensional superstructures could be placed symmetrically with respect to planar oxygen concentration c=0.25 (z=6.5), on the oxygen-lean side of the diagram. The resulting structures would be identical to those on the oxygen-rich side but with the roles of filled and empty chains interchanged. However, it is expected that ground states below about z=6.4 will not be observed experimentally because of slow kinetics resulting from the very low values of the tetragonal $\leftrightarrow$ orthorhombic transition in this region. One-dimensional ground states cannot form unless chains form by a tetragonal $\rightarrow$ orthorhombic transition. Chain morphology is symmetric (exchange of filled and empty parallel chains) about c=0.25. However, oxygen *site morphology* is symmetric about the central composition c=0.5 (z=7), so that the tetragonal $\leftrightarrow$ orthorhombic transition is highly asymmetric about c=0.25 (z=6.5). Hence, ordering on the oxygen-poor side of the phase diagram can be many orders of magnitude slower than on the oxygen-rich side because of much weaker thermodynamic driving force.

Much controversy surrounds the possible structures observed around z=6.35. Based on electron microscopy observations, Alario-Franco and co-workers [24] suggested the existence of an oxygen-ordered superstructure of tetragonal symmetry, of basal plane unit cell dimensions $2\sqrt{2}\ a_o \times 2\sqrt{2}\ a_o$, where a_o is the high-temperature tetragonal phase lattice parameter. The basal plane of this structure contains eight Cu atoms and three O atoms, so that its stoichiometry is z=6.375 (i.e., z=6+x, with x=3/8). Recent neutron diffraction work by Sonntag et al. [25] at first confirmed the existence of this postulated structure. These authors then concluded that theoretical phase diagram calculations should be extended to explain the observed superstructure. Such a conclusion is unwarranted: the suggested structure can only be stabilized if interaction $V_2>0$, which violates inequalities (1). In fact, the postulated structure contains a preponderance of energetically unfavorable 3-fold coordinated Cu atoms (see Fig. 3). In an even more recent publication [26] the investigators revised their analysis and proposed an orthorhombic unit cell containing isolated oxygen atoms. This new model is just as energetically unfavorable as the previous one, and for the very same reasons. As explained above, in *effective* pair interactions, Coulomb repulsion will tend to cancel out for large inter-oxygen spacings. At close distances, however, oxygens will always attract and bond via a Cu bridge. Therefore, randomly distributed O atoms in the YBCO basal plane, at equilibrium, will always form the longest possible chains if given enough time to migrate, thereby minimizing the number of energetically unfavorable chain-end configurations.

The conclusion is inescapable: whatever is being observed at these oxygen concentrations cannot possibly be ground states of oxygen order. Any attempt at force-fitting these types of structures into the phase diagram must result in internal contradictions and unphysical values of the parameters. Indeed, what would be required is a V_2 interaction which starts out positive around z=7, becomes negative around z=6.6, becomes positive again around z=6.5 (to stabilize the OII phase and associated long-period superstructures), then becomes negative once more around z=6.37. Such a scenario is hardly plausible, since it would require the energetically favorable Cu coordination to alternate back and forth between 3-fold and 2- and 4-fold configurations.

So, what is going on at x=3/8 (z=6.375)? At the oxygen-rich counterpart, x=5/8 (z=6.625), the predicted one-dimensional superstructure [21] is surely the correct ground state. The symbolic formula for its repeating unit is <11011010>, the 1's denoting filled, and the 0's denoting empty chains. This stoichiometric structure fulfills all the requirements: it contains only favorable Cu-coordination configurations and is strain-free (at least in isolated domains). Moreover, there is experimental evidence for its existence: faint electron diffraction peaks at reciprocal space points h=0.37 and equivalent have been observed [27], and the Fourier transform of <11011010> indeed has its most intense components at h=3/8=0.375 and equivalent [22]. For symmetry reasons, it is thus reasonable to expect that the "anti-structure" <00100101> must be the stable ordered ground state at the oxygen-lean composition x=3/8. Theoretically, at other oxygen stoichiometries, other long-period superstructures should form. If effective interactions are not sufficiently long-range, however, mixtures of one-dimensional structures are possible. In any case, a "row morphology" is expected, consisting of alternating filled and empty chains. If these row morphologies fulfill all ground state requirements, why have they not been observed experimentally to date at low oxygen content? Undoubtedly, these structures do not form because the driving force for oxygen ordering is far too low at oxygen-lean concentrations, due to the fact that the T→OI (chain formation) transition lies at very low temperatures.

The experimental observation that the "$\sqrt{2}$-structures" form at low oxygen content (close to the tetragonal phase boundary) but not at high oxygen content (deep inside the OI region) indicates quite clearly that these structures are metastable ones, since, as discussed above, tetragonal → orthorhombic ordering occurs at very low temperatures on the oxygen-lean side. Heating and cooling experiments in the electron microscope column [28] further confirm the metastable character of these structures. Moreover, if the diffraction contrast were due to oxygen ordering, one would expect significantly different diffraction patterns at each oxygen stoichiometry, but this is not observed. Diffraction data analysis based on correlated atomic displacements thus seems to be far more realistic, as suggested earlier by Krekels et al. [28]. A plausible scenario could then be the following: oxygen-lean YBCO samples at room temperature will tend to retain tetragonal symmetry, on average, containing short chains orthogonal to one another (see insert at the upper left of Fig. 2). Some short-range order is expected since orthogonal chain segments will tend to repel one another, *not* because of Coulomb interaction, but because of elastic interactions due to local orthorhombic distortions. The resulting elastic energy may then be reduced by modulated three-dimensional displacements, such as the rotation of oxygen coordination polyhedra centered on the CuO_2 plane [28]. As a result of these distortions, the system becomes locked into an average tetragonal (or micro-twinned orthorhombic) structure, thereby prohibiting evolution towards chain-like ground states upon further cooling.

In conclusion, thermodynamic stability analysis based on Coulomb repulsions is incorrect. Experimentally observed "$\sqrt{2}$-structures" cannot be ground states of order but must result from displacive transformations, not (directly at least) from oxygen ordering. True ground states will always consist, at equilibrium, of alternating full (O-Cu-O...) and empty (❑-Cu-❑...) infinite chains, as predicted by the ASYNNNI model. Only such "chain" structures must appear in an equilibrium phase diagram. Because of computational difficulties, thus far only Tetragonal, OI, $\overline{\text{OI}}$, OII and, more recently, OIII phase equilibria have been calculated. The resulting phase diagram, in its main features, is found to be relatively insensitive to the precise choice of effective interaction parameters, provided that inequalities (1) are satisfied for the dominant effective pair interactions. Elastic interactions play no role in determining equilibrium states in this system, although they may have an effect on metastable states like the "$\sqrt{2}$-structures". In addition, elastic distortions are responsible, for example, for diffuse [110] streaking observed in diffraction patterns of cation-substituted samples [29]. Other effects are described in a recent review by Suenaga et al. [30].

4. Tracer Diffusion

The asymmetry of the V_n interactions has important consequences for tracer diffusion in the YBCO compound, as shown in a recent Monte Carlo simulation investigation of the model system [31]. In this study, it was assumed that oxygen diffusion occurs by nearest neighbor thermally activated jumps, with constant energy barrier Q between equilibrium sites. Since "apical" (O4) oxygen sites are primarily occupied, diffusion is expected to be very much slower in the **c** than in the **a** and **b** directions, as observed experimentally [32].

In the chain plane of the orthorhombic phase, tracer diffusion should also be anisotropic. The experiment required to confirm this fact demands precise measurements on *detwinned* single crystals. This very difficult experiment has been performed recently by Rothman et al. [32], who reported significantly different diffusion rates along the **a** and the **b** directions, i.e., normal and parallel to the chains. The Monte Carlo simulation [31], which predated these experimental findings, correctly predicted this anisotropy and its cause, as will now be briefly summarized.

In crystals of orthorhombic symmetry, the tracer diffusion tensor $\mathbf{D}^*$ has three non-zero components, D^*_{11}, D^*_{22}, D^*_{33}. Let us consider only planar diffusion for which the tracer diffusivities are

$$D^*_{11} = \frac{\langle x^2 \rangle}{2t} \qquad \text{and} \qquad D^*_{22} = \frac{\langle y^2 \rangle}{2t} \tag{3}$$

where $\langle x^2 \rangle$ and $\langle y^2 \rangle$ are mean square displacements in the direction normal (**a**) and parallel (**b**) to the chains, respectively, and t is the elapsed time. We shall also consider the average

$$D^* = \frac{\langle x^2 + y^2 \rangle}{4t} \tag{4}$$

and the anisotropy factor

$$A = D^*_{11} / D^*_{22} \ . \tag{5}$$

The computation proceeds as follows [31]: A square lattice of 16×16 oxygen sites with periodic boundary conditions is used for the simulation. The model system is allowed to equilibrate during 10^4 MCS (Monte Carlo steps). Then, during a time ranging from 10^3 to 10^6 MCS, the positions of the O particles were recorded at regular time intervals and later used for the determination of mean-square displacements. The diffusivity tensors were then obtained from linear fits to the measured mean-square displacements as a function of time. During the simulation, the vacancy availability factor v and the jump probability w were also determined as ensemble averages. The tracer correlation factor f was back-calculated from the formula $D^* = \frac{1}{4}fvw$ [33].

Simulations were performed for four different temperatures (850, 950, 1050, 1150 K) and for planar oxygen concentrations ranging from c=0 all the way to c=1 (z=6.0 to z=8.0). Especially at the lower temperatures, D^* was found to vary over many orders of magnitude, having its lowest values sharply peaked around c=0.5 (z=7). The vacancy availability factor remained fairly constant from c=0 to c=0.5, then dropped rapidly, as expected, as c increased to unity. Also, as expected for constant pair interactions, the jump probability w was symmetric about c=0.5, at which it reached a minimum. The calculated correlation factor f had its expected value of unity at c=0 and tended to its theoretical value of f=0.467 for $c \rightarrow 1$ [35]. The anisotropy factor was, of course, unity for the tetragonal phase concentrations z=6 and

z=8, and reached a very sharp maximum at c=0.5 (z=7). At the lower temperature (850 K), in the fully ordered orthorhombic phase, the component D^*_{11} for diffusion along the chain was found to be about 10 times larger than the component D^*_{22} normal to the chains.

The activation energy E was determined through the Arrhenius form

$$D^* = D_0^* e^{-E/kt} \tag{6}$$

for various oxygen concentrations. The total activation energy is defined as $E = Q + \Delta H$ where ΔH is the energy change of the jump. Since the activation barrier Q is unknown, only the *variation* of E with concentration is meaningful. It was found that E increased by about 1 eV from c=0 (and c=1) to its sharp maximum at the central composition c=0.5.

The diffusivity anisotropy can be understood quite simply on the basis of the ASYNNNI model. Consider the well-ordered OI phase (Fig. 4a). For an interchange of two O atoms along the central chain, the system must reach the "activated state configuration" shown in Fig. 4b, whereas for an exchange of O atoms normal to the chains, the activated state shown in Fig. 4c must be reached. It is seen that activated state configurations b and c differ by an interchange of the roles of interaction parameters V_2 and V_3. A simple calculation indeed gives $\Delta H_a = 4V_1 - 2V + 4V_3$ and $\Delta H_b = 4V_1 + 4V - 2V_3$, where ΔH_a and ΔH_b are the energy differences between activated and ground states in the "a" and "b" configurations, respectively. The anisotropy would vanish, of course, for the "symmetric" model $V_2 = V_3$.

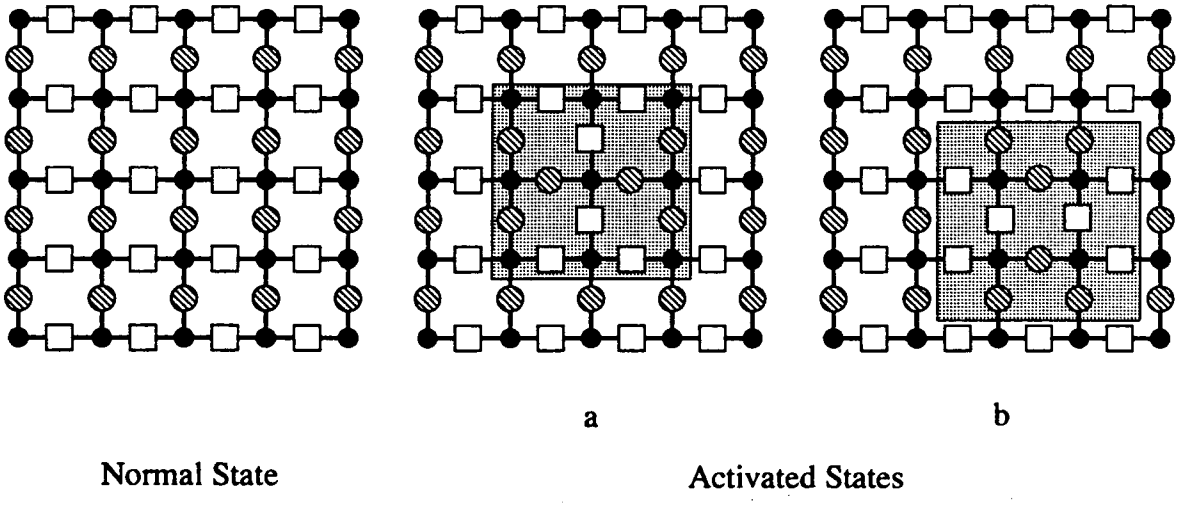

Figure 4 - Tracer oxygen diffusion in chain plane: (a) normal state (perfect OI at z=7), (b) activated complexes for diffusion along chain, and (c) normal to the chain.

5. Oxygen Order and Superconductivity

Earlier, it was conjectured [21] that the plateau structure observed in the variation of superconducting transition temperature (T_c) with oxygen content was at least partially due to the phenomenon of oxygen ordering. Experimentally, it was found by Farneth et al. [35] that the central T_c plateau for low-temperature vacuum-annealed samples of YBCO was sharply defined and entirely located at temperatures higher than the monotonically decaying T_c versus oxygen content curve for samples quenched from high temperatures. On the theoretical side, Lambin [36] used a tight-binding model to show that hole concentration for well-ordered OII and OIII phases should be higher than those for disordered compounds with the same oxygen concentration. Since, as was discussed above at some length, chain formation minimizes the fraction of incorrectly coordinated Cu ions (3-fold), it is tempting to correlate, at given oxygen concentration, optimal oxygen order and maximum T_c.

This conjecture received remarkable confirmation in the work of Argonne scientists on oxygen ordering at and below room temperature [37,38]. For quenched YBCO single crystals of oxygen content z=6.45, it was found that T_c increased markedly on subsequent aging, in fact by as much as 27 K. During this process, it was ascertained that oxygen content was not altered: the average occupancy on oxygen sites did not change, although the molar volume and lattice parameters contracted significantly, the **a** more than the **b**. Such behavior can only be interpreted as being due to *additional* oxygen ordering.

Recent "quench and age" Monte Carlo simulations [14] using the ASYNNNI model (with the V_1, V_2, V_3 parameters that were used in calculating the phase diagram of Fig. 2) have shed considerable light on the problem. Immediately after the instantaneous "computer quench," α/β ordering takes place during a very short transient, so short that it is probably unobservable experimentally. Subsequently, ordering of chain segments parallel to themselves, so as to form the longest possible chains, takes place at a rate characterized by a longer time constant.

The oxygen coordination of Cu1 atoms was monitored continuously during simulated aging at room temperature for samples quenched from 800 K. Electronic structure calculations [39] reveal that (spatially) 3- and 4-fold coordinated Cu (see Fig. 3) atoms are mostly present as Cu^{++}, and 2-fold coordinated Cu is present as Cu^{+}. As a result, chain "healing," i.e., progressive elimination of chain ends, where Cu is 3-fold coordinated, gives rise to the following "reaction" in Kröger-Vink notation:

$$2Cu_{3x} \rightarrow Cu_{4x} + Cu'_{2x} + h^{\bullet}$$

Chain healing thus creates holes ($h^{\bullet}$), accompanied by an excess negative charge on 2-fold coordinated Cu. The increasing hole concentration should favor a high T_c, but oxygen loss tends to destroy holes by the following mechanism:

$$O_O \rightarrow V_O + \tfrac{1}{2}O_2(g)$$
$$V_O^x \rightarrow V_O^{\bullet\bullet} + 2e'$$
$$2e' + 2h^{\bullet} \rightarrow \phi$$

The first of these three equations describes oxygen loss to the gas phase (g), the second describes ionization of vacancies and creation of electrons, the third describes electron-hole recombination. Chain healing is illustrated by examining the output of the Monte Carlo simulation of a z = 6.45 sample at two different times: immediately after the quench (Fig. 5a), and after annealing has taken place (Fig. 5b).

Monte Carlo simulations [14] clearly show that the fraction (f_{n-Cu}, with n=2, 3 or 4) of 2-fold or 4-fold coordinated sites increases with annealing time, and that of 3-fold sites decreases. These trends reproduce those of the rise in T_c observed experimentally by the Argonne group [37,38]. Moreover, since it is argued that oxygen ordering promotes hole formation, and that oxygen loss destroys holes, these two conflicting tendencies may well produce non-monotonic decay of T_c as oxygen content is decreased, possibly giving rise to the "plateaus" observed in the T_c vs. oxygen curve.

Recently, Poulsen et al. [40] were able to reproduce the observed plateau structure by a Monte Carlo procedure, much like the one reported here. Instead of monitoring Cu-coordination, these authors considered a relative population of two-dimensional "minimal-size clusters" of both Ortho I and Ortho II types. Upon careful analysis of their counting algorithm, it appears [41] that the good agreement with experiment obtained by Poulsen et al. is due to a very particular choice of rather artificial assumptions. It turns out that these authors have enough adjustable parameters in their formulation to fit any given two-plateau curve. Clearly, a more

physically meaningful approach was required. Our very recent efforts along those lines [41] will now be briefly summarized.

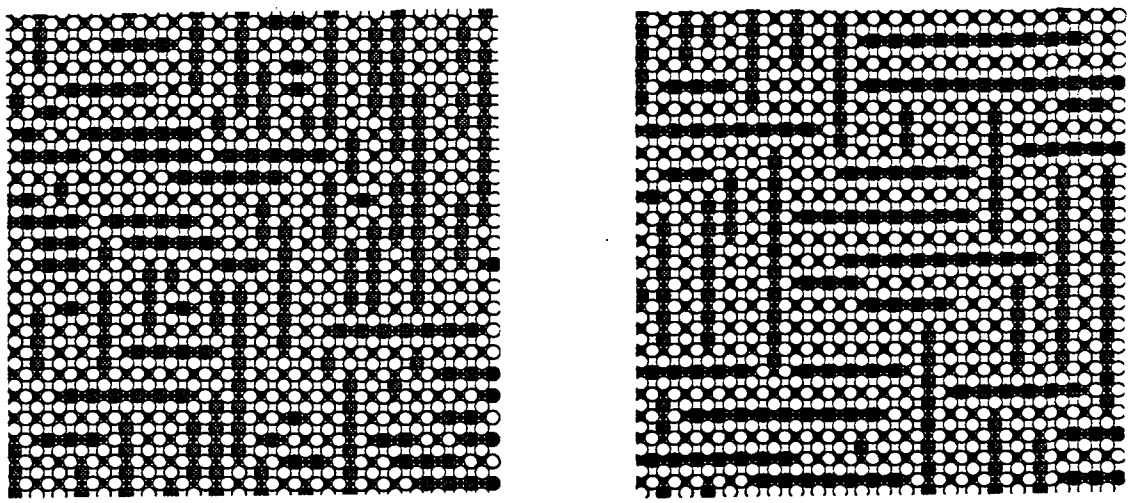

(a) (b)

Figure 5 - Monte Carlo output for a "quench and age" simulation at z=6.45. (a) Basal plane immediately following a quench from the tetragonal phase to the OII phase. Only short-range order exists at this point. (b) Basal plane after annealing for 100,000 MCS. Characteristic O-Cu-O chains have now formed, and OII order has been established.

Although not mentioned in Section 2, the derivation of Eq. (2) is based on the idea that *any* function of configuration in ordered or partially ordered systems can be expanded in a complete set of so-called *cluster functions* which may be defined in several ways [11,12]. In the present case, the function that we wish to expand is the hole count $h(\sigma)$, where σ denotes, symbolically, a certain configuration of O atoms on the sites of the two-dimensional lattice shown in Fig. 1. The coefficients of the expansion will be determined from the solution of a linear system (see below), and the oxygen configurations will be determined by Monte Carlo simulation.

The hole count at a given oxygen stoichiometry z is written as follows:

$$h(z) = \sum_{i=1}^{N} h_i f_i(z) \tag{7}$$

where the sum extends over the number of clusters (N) being used in the expansion; f_i represents the fraction of *copper* sites surrounded by the *oxygen/vacancy configuration* i (hereafter referred to as the *cluster probability*), and h_i is the "hole coefficient" for that configuration. This study uses a cluster figure which consists of two unit cells in the basal plane, and contains 8 oxygen and 3 copper sites. The number of configurations considered on this cluster is 14: 6 ordered and 8 disordered. "Ordered" clusters are considered to be the cluster distinct by symmetry which are composed of only O-Cu-O and/or ❑-Cu-❑ chains; "disordered" clusters are all other configurations on the chosen 8-point cluster figure. This distinction between ordered and disordered clusters is not essential to the method, it is only used for simplicity. The configurations used are shown in Fig. 6, and will be referred to hereafter using the designations given in column three. Clusters C_1 to C_6 in Fig. 6 are the ordered clusters and D_1 to D_8 are the disordered clusters. The copper atom which is used in the given configuration is the central atom, depicted by a small black circle in Fig. 6 (column 1).

The hole coefficients h_i in Eq. (7) are found by using electronic structure parameters calculated by Lambin [36]. The results of Lambin are particularly useful in our study since he calculates hole counts for four ordered superstructures and for several disordered structures. The hole coefficients are then found by solving a system of linear equations generated using Eq. (7). After obtaining the correct number of equations, the system is solved by simple matrix inversion. To generate these equations, we need to determine the cluster probabilities of a set of structures for which the hole count has been computed. This was done for four perfectly ordered structures and for a set of artificially generated "disordered" structures. Unfortunately, the structures selected make the matrix of the linear system ill-conditioned, so that the method of singular value decomposition must be used. The values of hole coefficients h_i obtained by this method [41] are given in the last column of Fig. 6.

Cluster	Description	Designation	Hole Coefficient
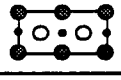	3 Chains	C_1	0.25
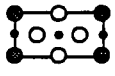	2 Chains	C_2	0.18
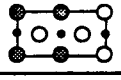		C_3	0.16
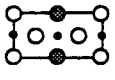	1 Chain	C_4	0.096
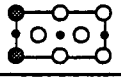		C_5	-0.010
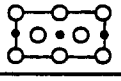	0 Chains	C_6	-0.02
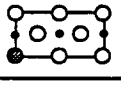	Disord. (1)	D_1	-0.12
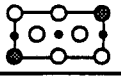	Disord. (2)	D_2	-0.29
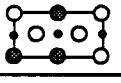	Disord. (3)	D_3	-0.15
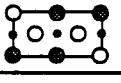	Disord. (4)	D_4	0.094
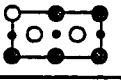	Disord. (5)	D_5	0.19
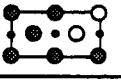	Disord. (6)	D_6	0.48
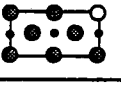	Disord. (7)	D_7	-1.25
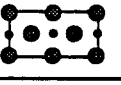	Disord. (8)	D_8	0.046

Figure 6 - Configurations used in cluster expansion. Clusters are shown in column 1, with a brief description given in column 2. Column 3 gives the designations used throughout the paper, and column 4 indicates the hole coefficients used in the cluster expansion.

Monte Carlo simulations are now performed for different stoichiometries from z=6 to z=7 at a temperature 300 K until states of near equilibrium are attained. Each simulation was performed in the grand canonical ensemble using a 64x64 lattice (4096 sites) with periodic boundary conditions. The interactions used were the same V_1, V_2, V_3 as were used for the phase diagram calculation, plus an additional repulsive interaction, $V_4 = 0.17\ V_3$ (third neighbor along the direction of V_3). The simulations were carried out for 1100 MCS, where one MCS involves attempting a spin flip on every site in the lattice, i.e., an exchange of O to ❑ or conversely. Monte Carlo simulations were performed at the temperature of 300 K, at which all of the ordered phases of interest (OI, OII, OIII and $\overline{\text{OI}}$) are stable. At each concentration, the fraction f_i of Cu sites which exist in the configurations listed in Fig. 5 are recorded. Then, by direct application of Eq. (7), the hole counts h(z) are determined for these simulated configurations.

The resulting values h(z) are plotted as a function of z in Fig. 7. The relative contributions from the "ordered" (full circles) and "disordered" (open circles) configurations are shown in Fig. 6a and the total hole count, which is the sum of these two contributions, is plotted in Fig. 6b (filled circles). Hole count for completely disordered states (having no short-range correlations) is also shown in Fig. 6b as open circles. As expected, the h(z) curve for ordered states lies entirely above that for disordered states. Moreover, the ordered state curve displays the semblance of a plateau around z=6.6. The experimentally determined two-plateau feature of the T_c versus z curve is not well reproduced, however: the theoretical z=6.6 "plateau" is not very flat, and there is no flattening at all around z=7. It must therefore be concluded that the relationship between h(z) and $T_c(z)$ is not a simple one and that the two T_c plateaus probably have different origins. The one near 6.6 may well be due to the influence of oxygen ordering but the one near 7.0 is probably due to saturation effects, as discussed for example by Tokura et al. [43].

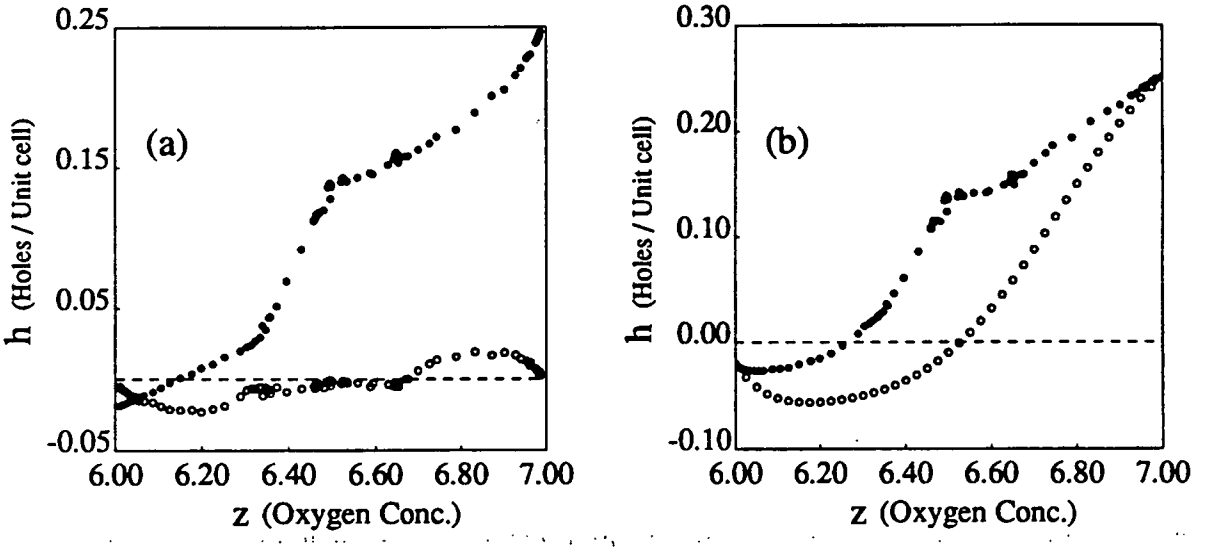

(a) (b)

Figure 7 - Hole counts predicted using the cluster expansion method. (a) Relative contributions to the total hole count from ordered configurations (filled circles) and disordered configurations (open circles). (b) Total hole count (filled circles) found using cluster probabilities generated by Monte Carlo simulation. Open circles show the total hole count for structures which are disordered on the O(1) sublattice.

6. Conclusion

The ASYNNNI model is the simplest one which correctly accounts for the main features of oxygen ordering in YBCO. Predicted ground states and the related phase diagram are in excellent agreement with available experimental evidence, provided that one distinguishes carefully between stable and metastable states. The asymmetry in properties, such as the equilibrium chain morphology or the diffusivity anisotropy, is a direct consequence of the asymmetry of the second neighbor effective oxygen pair interactions. That asymmetry, in turn, is a consequence of the requirement of correct O-coordination of Cu in the chain plane. The elimination of unfavorable 3-fold coordination, or "chain healing", may occur by low-temperature diffusion in off-stoichiometric samples, thereby raising T_c in the course of an annealing treatment. In conclusion, despite its simplicity, the ASYNNNI model has been highly successful in predicting, explaining or rationalizing a variety of phenomena observed in the high-T_c superconducting compound $YBa_2Cu_3O_z$.

Acknowledgments

This work was supported by the Director, Office of Energy Research, Office of Basic Energy Sciences, Materials Sciences Division of the U.S. Department of Energy under Contract No. DE-AC03-76SF00098. The authors are grateful to Mr. Mark Asta, Dr. S. C. Moss, and Dr. G. Van Tendeloo for many helpful discussions.

References

1. D. de Fontaine, L. T. Wille, and S. C. Moss, Phys. Rev. B, 36 (1987), 5709-5712.
2. L. T. Wille and D. de Fontaine, Phys. Rev. B, 37 (1988), 2227-2230.
3. J. Stolze, Phys. Rev. Lett., 64 (1990), 970-973.
4. P. Sterne and L. T. Wille, Physica C, 162 (1989), 223-224.
5. V. E. Zubkus, S. Lapinskas, and E. E. Tornau, Physica C, 159 (1989), 501-509.
6. R. Kikuchi and J. S. Choi, Physica C, 160 (1989), 347-352.
7. G. Ceder et al., Phys. Rev. B, 41 (1990), 8698-8701.
8. N. H. Andersen, B. Lebech, and H. F. Poulsen, J. Less-Common Metals, 164-165 (1990), 124-131.
9. D. K. Hilton et al., preprint (1991).
10. J. M. Sanchez, F. Ducastelle, and D. Gratias, Physica, 128A (1984), 334-350.
11. M. Asta et al., Phys. Rev. B, 44 (1991), 4907-4913.
12. C. Wolverton et al., Phys. Rev. B, 44 (1991), 4914-4924.
13. J. K. Burdett and G. V. Kulkarni, Phys. Rev. B, 40 (1989), 8708-8932.
14. G. Ceder, R. McCormack, and D. de Fontaine, Phys. Rev. B, 44 (1991), 2377-2380.
15. A. G. Khachaturyan, S. V. Semenovskaya, and J. W. Morris, Jr., Phys. Rev. B, 37 (1988), 2243-2246.
16. A. G. Khachaturyan and J. W. Morris, Jr., Phys. Rev. Lett., 61 (1988), 215-218.

17. S. V. Semenovskaya and A. G. Khachaturyan, Phys. Rev. Lett., 67 (1991), 2223.

18. A. A. Aligia, A. G. Rojo, and B. R. Alascio, Phys. Rev. B, 38 (1988), 6604.

19. T. Aukrust et al., Phys. Rev. B, 41 (1990), 8772.

20. A. G. Khachaturyan and J. W. Morris, Jr., Phys. Rev. Lett., 61 (1988), 215-218.

21. D. de Fontaine, G. Ceder, and M. Asta, Nature, 343 (1990), 544-546.

22. G. Ceder, M. Asta, and D. de Fontaine, Physica C, 177 (1991), 106-114.

23. D. de Fontaine, M. E. Mann, and G. Ceder, Phys. Rev. Lett., 63 (1989), 1300-1303.

24. M. A. Alario-Franco et al., Physica C, 156 (1988), 455.

25. R. Sonntag et al., Phys. Rev. Lett., 66 (1991), 1497-1500.

26. Th. Zeiske et al., Z. Phys. B, 86 (1992), 11-15.

27. R. Beyers et al., Nature, 340 (1989), 619-621.

28. T. Krekels et al., Physica C, 167 (1990), 677-690.

29. X. Jiang et al., Phys. Rev. Lett., 67 (1991), 2167.

30. Yimei Zhu, J. Tafto, and M. Suenaga, MRS Bull., 16 (1991), 54-59.

31. E. Salomons and D. de Fontaine, Phys. Rev. B, 41 (1990), 11159-11167.

32. S. J. Rothman et al., Phys. Rev. B, 44 (1991), 2326.

33. G. E. Murch, Philos. Mag. A, 41 (1980), 157.

34. A. D. LeClaire in Physical Chemistry, Vol. 10, ed. H. Eyring, D. Henderson, and W. Just (New York, NY: Academic Press, 1970).

35. W. E. Farneth et al., Solid State Commun., 66 (1988), 953-959.

36. Ph. Lambin, "Tight-Binding Investigation of the Electronic Properties of Ordered and Disordered Defects in the YBaCuO System," Oxygen Disorder Effects in High T_c Superconductors, ed. J. L. Morán-López and Ivan K. Schuller (New York, NY: Plenum Press, 1990), 101-116.

37. B. W. Veal et al., Phys. Rev. B, 42 (1990), 4770-4773.

38. J. D. Jorgensen et al., Physica C, 167 (1990), 571-578.

39. A. Latgé, E. V. Anda, and J. L. Morán-López, Phys. Rev. B, 42 (1990), 4288-4297.

40. H. F. Poulsen et al., Nature, 349 (1991), 594-596

41. R. McCormack, G. Ceder, and D. de Fontaine, submitted to Phys. Rev. B.

42. Y. Tokura et al., Phys. Rev. B, 38 (1988), 7156.

LAWRENCE BERKELEY LABORATORY
UNIVERSITY OF CALIFORNIA
TECHNICAL INFORMATION DEPARTMENT
BERKELEY, CALIFORNIA 94720